

Transcutaneous Spinal Direct Current Stimulation

Modelling the Electric Field Distribution in the Cervical Spinal Cord

S. R. Fernandes^{1,2}, R. Salvador¹, C. Wenger¹, M. de Carvalho² and P. C. Miranda¹

¹*Institute of Biophysics and Biomedical Engineering (IBEB), Faculdade de Ciências,
Universidade de Lisboa, 1749-016 Lisboa, Portugal*

²*Molecular Medicine Institute (IMM), Faculdade de Medicina, Universidade de Lisboa,
Avenida Professor Egas Moniz, 1649-028, Lisboa, Portugal*

1 OBJECTIVES

Following the reports that weak electrical currents can modulate excitability in cortical areas, Cogiamanian et al. (2012) proposed that the same approach could be applied to modulate spinal cord function. Exploratory studies in humans showed that transcutaneous spinal direct current stimulation (tsDCS) has neuromodulatory effects on spinal motor circuitry (e.g. Bocci et al., 2014). There is currently only one computational study of the electric field distribution during tsDCS applied on the thoracic spine region that has been published, which applies realistic human models based on high-resolution MRI of healthy volunteers (Parazzini et al., 2014). There are no known tsDCS modelling studies on human cervical spine, so there is a need to develop human realistic models to solve for the field distribution in cervical spine stimulation.

The main objective of the present study is to perform a finite element analysis (FEA) of the electric field distribution in tsDCS in the cervical spine region, and refer to cervical spine circuitry that may be modulated by tsDCS in order to address viability for clinical application purposes.

2 METHODS

The 34 year-old Duke model, from the Virtual Population Family v1.x models (Christ et al., 2010), was used to generate volume meshes for FEA with MIMICS (v16, <http://www.materialise.com/mimics>). From this model, eight tissues were selected: skin, fat (including subcutaneous adipose tissue), muscle, bone and vertebrae, intervertebral disks, dura mater, cerebrospinal fluid (CSF) and spinal cord.

The electrode configuration tested followed the experimental setup considered in Bocci et al. (2015): the target electrode was placed over the C6-T1 spinous

processes; the return electrode was placed over the right deltoid muscle, in a site far from the target. The electrodes were modelled as 5x7 cm² rectangular sponges soaked in saline solution ($\sigma=2$ S/m (Miranda, Mekonnen, Salvador and Ruffini, 2013)), with a thickness of 3 mm thick, between electrode and skin surfaces. Electric conductivity value of all tissues were based on data found in literature for DC currents: $\sigma_{\text{skin}} = 0.435$ S/m; $\sigma_{\text{fat}} = 0.040$ V/m; $\sigma_{\text{muscle}} = 0.355$ S/m (average between muscle transverse (0.043 S/m) and muscle longitudinal conductivity (0.667 S/m) values from Rush, Abildskov and McFee, 1963); $\sigma_{\text{vertebrae/bone}} = 0.006$ S/m; $\sigma_{\text{intervertebral disks}} = 0.200$ S/m; $\sigma_{\text{dura mater}} = 0.03$ S/m; $\sigma_{\text{CSF}} = 1.79$ S/m; $\sigma_{\text{spinal cord}} = 0.154$ S/m (Geddes and Baker, 1967; Rush, Abildskov and McFee, 1963; Hauelsen, Ramon, Eiselt, Brauer and Nowak, 1997; Baumann, Wozny, Kelly and Meno, 1997; Struijk, Holsheimer, Barolat, He and Boom, 1993). COMSOL Multiphysics (version 4.3b, www.comsol.com) was used to calculate the electric field distribution using FEA. The current intensity in the electrodes was set to 2.5 mA, as in previous studies (Bocci et al., 2014). The boundary conditions were applied according to Miranda et al. (2013).

3 RESULTS

Figure 1 presents the electric field magnitude distribution along the spinal cord. Figure 1a) shows the volume-weighted average along the z axis, considering slices of the spinal cord with 1 mm height. This curve has two peaks in the region of the spinal segments C5-T1 (corresponding to the braquial plexus), with values of 0.171 V/m ($z = [1570; 1571]$ mm) and 0.186 V/m ($z = [1587; 1588]$ mm). Figure 1b) shows the electric field magnitude volume distribution in the spinal cord, where it can be seen that these and other local maxima in the field distribution are found in regions where the vertebral

canal is narrowed due to the intrusion of intervertebral disks or vertebrae body's edges.

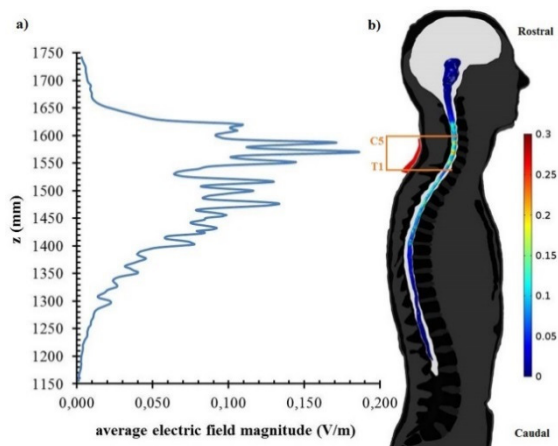


Figure 1: a) Volume-weighted average electric field magnitude distribution along the z axis; b) Electric field magnitude volume distribution colour plot in the spinal cord, including a background representation of anatomical structures, the target electrode (in red) and the position of the brachial plexus spinal segments C5-T1 (in orange).

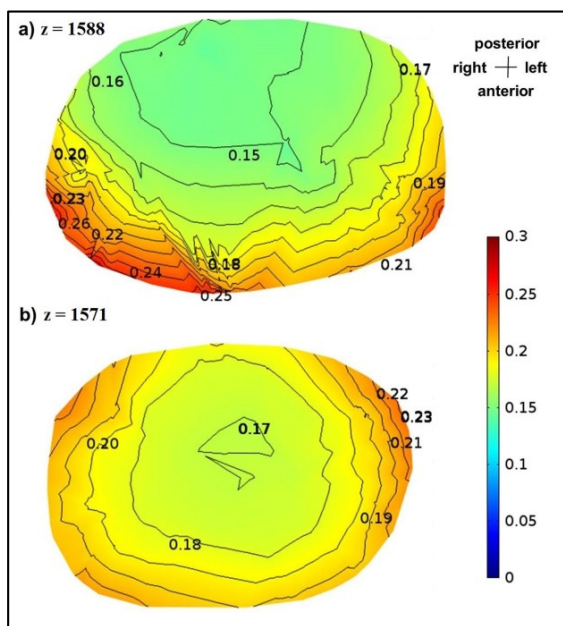


Figure 2: Contour plots of the electric field magnitude (V/m) in the spinal cord in two axial slices: a) $z=1588$ mm; b) $z=1571$ mm. The anatomic orientation and the colour scale (in V/m) are presented on the right.

Figure 2 presents two contour plots of the electric field distribution in the spinal cord at the level of the two highest peaks in fig. 1a). In Figure 2a), the maximum values reach 0.26 V/m and are located in the anterolateral region of the spinal cord, with an

asymmetric distribution with a larger maximum magnitude region on the right. This could be due to the position of the return electrode, influencing the electric field lines direction. Figure 2b) presents a more symmetric distribution, with maximum field magnitude values on the posterolateral region of the spinal cord, reaching a maximum of 0.23 V/m. The fact that Figure 1a) presents an average distribution accounts for the difference in maximum value peaks when comparing with Figure 2.

Values of the ratio between the magnitudes of the normal and tangential components to the spinal cord surface as function of position along the z axis are presented in Figure 3. The values calculated span between 1.5 and 20.2, which means that the tangential component is higher than the normal component, resulting in an electric field direction preferentially tangential to the spinal cord.

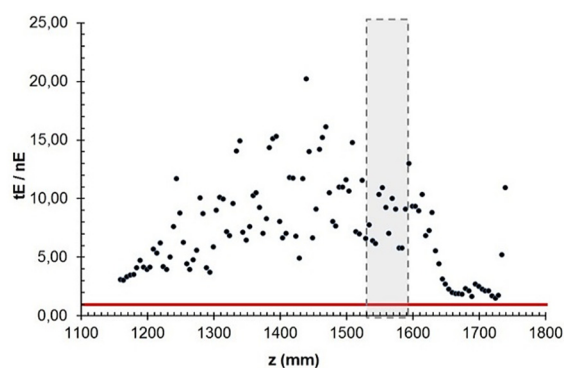


Figure 3: Ratio between the magnitudes of the tangential and normal components of the electric field along the z axis in the spinal cord. The red horizontal line corresponds to a ratio of 1 (equal magnitude of both components). The region of the segments C5-T1 is marked in grey.

4 DISCUSSION

In modelling studies of tDCS, based on the stimulation conditions applied to the motor cortex in clinical studies with neuromodulatory effects reported, electric field magnitudes of 0.15 V/m and above were registered (Miranda et al. 2013). In the present study, the electric field magnitude distribution presented values above 0.15 V/m in the upper region of the spinal segments C5-T1. As this region is related to upper limb function (braquial plexus), this may indicate that the values reached can be sufficient for neuromodulatory effects on upper limb neurological functions. Figure 2a) presents maximum values in the anterolateral region of the spinal cord. This region is

related with sensory ascending tracts, responsible for proprioception (spinocerebellar tracts), traditional senses (spinothalamic tracts), and motor subconscious descending tracts that regulate balance, muscle tone, eye, hand and upper limb position. In Figure 2b), the maximum values are located mainly on the posterolateral region, related to tracts that regulate conscious (posterior and lateral costicospinal tracts) and subconscious (rubrospinal tracts) control of skeletal muscles. These results are in agreement with exploratory clinical tsDCS studies, that show modulation of nociceptive ascending pathways and spinal motor circuitry, depending on electrode polarity, when stimulating thoracic and cervical spine regions (Cogiamanian et al., 2012; Hubli, Dietz, Schrafl-Altarmatt and Bollinger, 2013; Bocci et al., 2014). In particular, cervical cathodal tsDCS had an increasing effect in motor unit recruitment and decreased peripheral silent period in respect to sham and anodal conditions (Bocci et al., 2014).

In the present study, the electric field in the spinal cord had a larger tangential electric field component along the spinal cord. As the electric field is directly proportional to the current density, this may be in agreement to the results of the modelling study by Parazzini et al. (2014), in which the current density direction in the spinal cord was mostly longitudinal during thoracic tsDCS.

One shortcoming of the present model is the low number of tissues, considering only the ones closer to the target electrode. A more complete model could reveal more about spreading effects on the electric field. Also, the muscle conductivity value was taken as an average between transverse and longitudinal values in the literature, so anisotropic data could be valuable in future studies. In spite of these limitations, the results are in agreement with previous modelling and experimental results.

Cervical tsDCS is a promising non-invasive clinical tool for neuronal circuitry modulation in the cervical spinal cord. It could address neuronal dysfunctions like spasticity, present in many neurologic diseases (e.g. amyotrophic lateral sclerosis). Defining accurate models that predict the physical effects of tsDCS on spinal neurons could be a powerful tool to develop clinical applications more focused on the specific neurologic patient needs.

ACKNOWLEDGEMENTS

This research was supported in part by the

Foundation for Science and Technology (FCT), Portugal. S. R. Fernandes was supported by a FCT grant, reference SFRH/BD/100254/2014. C. Wenger was supported by Novocure.

REFERENCES

- Baumann, S. B., Wozny, D., Kelly, S., Meno, F. (1997). The electrical conductivity of human cerebrospinal fluid at body temperature." *IEEE Transactions on Biomedical Engineering*, 44(3):220-223.
- Bocci, T., Vanninia, B., Torzini, A., et al. (2014). Cathodal transcutaneous spinal direct current stimulation (tsDCS) improves motor unit recruitment in healthy subjects. *Neuroscience Letters*, 578:75–79.
- Christ, A., Kainz, W., Hahn, E. G., et al. (2010). The Virtual Family-development of surface based anatomical models of two adults and two children for dosimetric simulations. *Phys. Med. Biol.*, 55:N23–N38.
- Cogiamanian, F., Ardolino, G., Vergari, M., et al. (2012). Transcutaneous spinal direct current stimulation. *Frontiers in Psychiatry*, 3, article 63.
- Geddes, L.A. and Baker, L.E. (1967). The specific resistance of biological materials – a compendium of data for the biomedical engineer and physiologist. *Med. & Biol. Eng.*, 5:271 – 293.
- Hauseisen, J., Ramon, C., Eiselt, M., Brauer, H., Nowak, H. (1997). Influence of tissue resistivities on neuromagnetic fields and electric potentials studied with a finite element model of the head. *IEEE Trans. Biomed. Eng.*, 44:727-735.
- Hubli, M., Dietz, V., Schrafl-Altarmatt, M., Bollinger, M. (2013). Modulation of spinal neuronal excitability by spinal direct currents and locomotion after spinal cord injury. *Clinical Neurophysiology*, 124: 1187-1195.
- Miranda, P.C., Mekonnen, A., Salvador, R., Ruffini, G. (2013). The electric field in the cortex during transcranial current stimulation. *Neuroimage*, 70:48-58.
- Parazzini, M., Fiocchi, S., Liorni, I., et al. (2014). Modelling the current density generated by transcutaneous spinal direct current stimulation (tsDCS). *Clinical Neurophysiology*, 125(11):2260-70.
- Rush, S., Abildskov, J.A., McFee, R. (1963). Resistivity of body tissues at low frequencies. *Circulation Research*, 12:40-50.
- Struijk, J. J., Holsheimer, J., Barolat, G., He, J., Boom H.B.K. (1993). Paresthesia thresholds in spinal cord stimulation: a comparison of theoretical results with clinical data. *IEEE Trans. Rehab. Eng.*, 1:101–108.